

Latent Regularization in Generative Test Input Generation

Giorgi Merabishvili

gmerabi@ncsu.edu

North Carolina State University

USA

Oliver Weißl

weissl@fortiss.org

Technical University of Munich &

fortiss GmbH

Germany

Andrea Stocco

andrea.stocco@tum.de

Technical University of Munich &

fortiss GmbH

Germany

Abstract

This study investigates the impact of regularization of latent spaces through truncation on the quality of generated test inputs for deep learning classifiers. We evaluate this effect using style-based GANs, a state-of-the-art generative approach, and assess quality along three dimensions: validity, diversity, and fault detection. We evaluate our approach on the boundary testing of deep learning image classifiers across three datasets, MNIST, Fashion MNIST, and CIFAR-10. We compare two truncation strategies: latent code mixing with binary search optimization and random latent truncation for generative exploration. Our experiments show that the latent code-mixing approach yields a higher fault detection rate than random truncation, while also improving both diversity and validity.

CCS Concepts

- Software and its engineering → Software verification and validation.

Keywords

Deep learning testing, test generation, truncation, generative AI

ACM Reference Format:

Giorgi Merabishvili, Oliver Weißl, and Andrea Stocco. 2026. Latent Regularization in Generative Test Input Generation. In *7th International Workshop on Deep Learning for Testing and Testing for Deep Learning (DeepTest '26) (DeepTest '26), April 12–18, 2026, Rio de Janeiro, Brazil*. ACM, New York, NY, USA, 8 pages. <https://doi.org/10.1145/3786154.3788585>

1 Introduction

Testing deep learning (DL) systems requires large, diverse, and valid inputs to expose misbehaviors [10, 11, 14, 21–23, 25, 29–31, 37–43, 47]. As deep learning models and datasets grow in complexity, manually creating such inputs becomes infeasible due to the huge size of the input space. Test input generators can be used to sample from this space more effectively. Recent generative AI methods, such as style-based GANs, are promising as they produce high-quality synthetic data and enable structured manipulations in their latent spaces [9, 17, 18]. Generating test inputs requires balancing two conflicting objectives: the inputs should be valid (plausible and human-recognizable) but also diverse enough to explore the DL system decision space and reveal faults.



This work is licensed under a Creative Commons Attribution 4.0 International License.

DeepTest '26, Rio de Janeiro, Brazil

© 2026 Copyright held by the owner/author(s).

ACM ISBN 979-8-4007-2386-5/2026/04

<https://doi.org/10.1145/3786154.3788585>

Previous work has used GANs to generate test inputs with semantic variations (for example, weather changes in autonomous driving) [48], using mechanisms such as *truncation* to balance realism and diversity [4, 26]. Truncation works by moving latent codes toward their mean, producing more realistic but less diverse images. Although truncation is part of most modern GANs [35], its effect on generating test inputs for DL systems has not been thoroughly analyzed. Existing DL testing work usually relies on pixel or feature perturbations [11, 30], or explores semantic changes without considering truncation as a controllable factor [43, 48]. Recent search-based approaches [7, 16, 32, 45, 50, 51] explore other forms of variability, but not this specific trade-off.

This work explores how truncation, a common latent-space regularization method, influences the quality of test inputs produced by class-conditional StyleGAN2 models. These models form the foundation of recent generative testing frameworks, such as MIMICRY [45], which we adopt as a reference in this study. We first perform a screening step on the generated input seeds to filter out invalid samples, using a combination of classifier confidence, output margin, SSIM, and ℓ_2 threshold [13, 20, 33, 34]. We further evaluate an adaptive truncation strategy, in which we progressively decrease the truncation rate until valid candidate seeds are produced. These “salvaged” seeds typically lie close to the classifier’s decision boundaries and are therefore more likely to trigger misclassifications. Using these seeds, we then generate failure-inducing inputs with Mimicry through a search-based test generation procedure.

We conduct experiments on three datasets, namely MNIST, Fashion MNIST, and CIFAR-10, varying the truncation level to study its effect on multiple quality metrics: (i) the proportion of samples passing automatic screening, (ii) the fraction of human-validated valid samples, (iii) the diversity among validated samples, and (iv) the fault detection rate among validated inputs.

Our experiments demonstrate the advantage of the adaptive seed selection strategy. In the MNIST benchmark targeting 25 frontier pairs, 15 samples were confirmed as valid and fault-revealing, with 12 of them originating from salvaged seeds. Overall, our results indicate that adaptive truncation improves the acceptance of generated test inputs while maintaining high diversity and increasing fault detection effectiveness.

Our experiment revealed that mild–moderate latent regularization ($\psi \approx 0.6$) maximizes human-validated frontier yield on MNIST. The adaptive policy minimizes human effort (seeds/valid) by salvaging hard seeds. Qualitative analysis shows that diversity remains adequate at these settings to expose faults, whereas overly strong regularization offers lower returns. First-flip is the most efficient for fault discovery under latent regularization; *style-mixing* complements it by adding semantic control over boundary direction. Using

first-flip to triage seeds (possibly with adaptive ψ) and *style-mixing* provides strong overall coverage of boundary behaviors.

Our paper makes the following contributions:

Systematic study of truncation for test generation. We conduct the first structured investigation of how latent-space regularization through truncation affects the quality of generated test inputs for deep learning classifiers.

Adaptive truncation strategy for seed selection. We propose an adaptive truncation method that progressively lowers the truncation parameter ψ to salvage seeds near decision boundaries, improving fault discovery and diversity.

Experimental evaluation. We evaluate both random and search-based truncation strategies on three datasets, MNIST, Fashion MNIST, and CIFAR-10, measuring validity, diversity, and fault detection under different truncation levels. Our experiments show that adaptive truncation improves the acceptance rate and fault detection capability of generated test inputs, offering practical guidance for designing generative testing frameworks.

2 Background

2.1 DL Testing Objectives

Testing of DL systems generally serves two goals: *robustness testing*, which stresses a trained model using semantically preserved perturbations, and *generalization testing*, which seeks novel yet *valid* inputs that traverse or expose decision boundaries [11, 25, 30, 43, 47].

Boundary testing is a form of generalization testing that focuses on regions of near-ambiguity [44], where class confidences are similar. It can be performed in an *untargeted* way (searching for any label flip) or *targeted* (moving from a source class toward a specific rival suggested by the model’s confidence distribution). Targeted exploration is usually more sample-efficient in high-dimensional spaces, as it constrains the search to a source–rival corridor on the decision surface [3, 5, 27, 45].

2.2 Test Input Generation Families

Existing DL testing approaches can be broadly grouped into input-based, model-based, and latent-space methods. Input-based techniques perturb existing samples directly in the input space, for example, via gradient-based approaches such as DeepXplore [30] and DLFuzz [11], or random and search-based transformations [43]. While simple and model-agnostic, these methods mainly target robustness testing and offer limited control over semantic validity. Model-based methods instead explore explicit domain abstractions to generate challenging yet valid inputs [6, 32, 50, 51], but their effectiveness depends on the fidelity of the underlying model.

Latent-space methods aim to provide realistic inputs using a generative model and explore its latent space to produce diverse, semantically plausible test cases [8, 16, 45]. Recent GenAI-based frameworks, including MIMICRY [45], RBT4DNN [28], CIT4DNN [7], and GIFTBENCH [26], use different forms of latent-space exploration, including interpolation, noise injection, and guided search, to generate semantically valid and behavior-revealing test inputs.

In this work, we focus on latent-space methods and isolate the role of a single, widely used control parameter—*truncation*—as a factor influencing the validity, diversity, and fault-revealing power

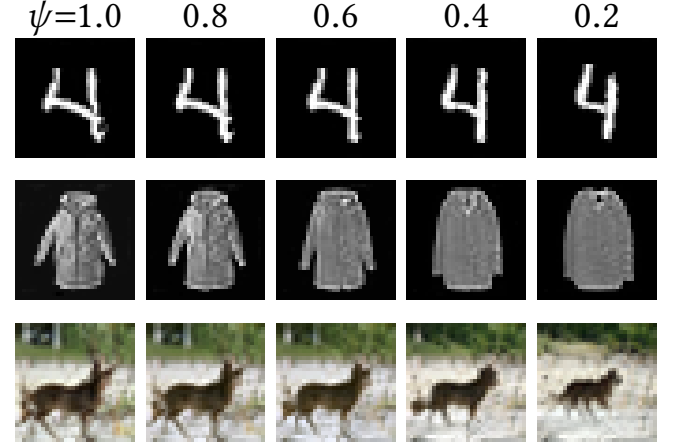


Figure 1: Truncation on coarse layers. A fixed latent seed at $\psi = 1.0$ and progressively lower ψ values increase fidelity and reduce diversity.

of generated test inputs. Our study builds on MIMICRY, which serves as the reference generator for all experiments.

MIMICRY uses a class-conditional StyleGAN to structure the latent space into an intermediate representation \mathcal{W} , obtained by mapping an initial latent vector $z \in \mathcal{Z}$. This representation supports layer-wise control and semantic manipulation via style or feature mixing [2, 15, 18, 36, 45]. Test generation is formulated as a search for *boundary inputs*, i.e., samples located near the decision boundary of the system under test, where class confidences are balanced. We leverage this framework to study how truncation reshapes the latent space during boundary exploration.

3 Methodology

In generative test input generators such as MIMICRY, the truncation parameter ψ can be used as a regularization control that moves each latent code toward the average latent \bar{w} , trading diversity for realism. The so-called *truncation trick* contracts latent codes w toward the running average \bar{w} according to:

$$w' = \bar{w} + \psi(w - \bar{w}), \quad \psi \in (0, 1].$$

Lower values of ψ typically increase visual realism and classifier confidence but reduce the diversity of generated samples [4, 35]. This makes truncation a natural variable for studying how fidelity controls influence the generation of valid and fault-revealing test inputs. However, test input generation must also balance other competing goals: *validity*, i.e., producing class-plausible images, and *diversity*, i.e., covering enough of the input space to traverse decision boundaries and expose faults.

Truncation in StyleGAN can be applied uniformly across all layers in the latent code w or on a per-layer basis in \mathcal{W}^+ []. Uniform schedules simplify comparisons, while layer-wise schedules allow different truncation values per layer to preserve coarse semantic structure [2, 18, 36]. Lowering the truncation parameter ψ concentrates samples in high-density regions, typically increasing fidelity and classifier confidence while reducing diversity. An example is given in Fig. 1.

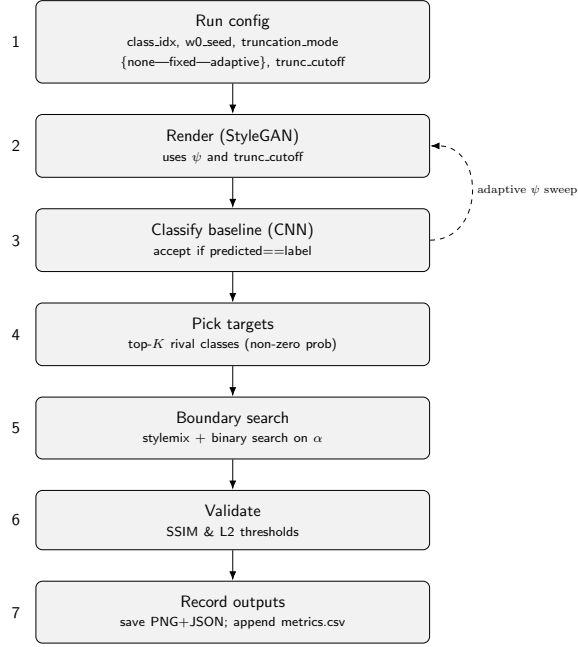


Figure 2: Test input generation with truncation workflow.

3.1 Approach

We use two key notions throughout our approach. The *minimal acceptable truncation* ψ^* is the smallest ψ at which a seed remains behavior-preserving for the system under test (SUT); this forms the basis of *seed salvage*. The *first-flip truncation*, instead, is the first ψ (descending from 1.0) at which the SUT prediction changes.

Our test input generation workflow is illustrated in Fig. 2. Each run is configured with a class index, latent seed, truncation mode (*none*, *fixed*, *adaptive*), and truncation cutoff, specifying the feature layer up until truncation will be applied, starting from the bottom, giving an option to truncate only lower layers and leave fine details unchanged. Images are rendered at the chosen ψ with the initial latent z frozen to isolate truncation effects [1]. The baseline check at $\psi = 1.0$ ensures that only seeds passing the fixed confidence and margin requirements are retained. For boundary testing, we select the top- K rival classes according to the DL classifier probabilities whenever we have non-zero probabilities for classes other than the source [32]. Each candidate then undergoes boundary exploration using one of two techniques: truncation-assisted style mixing or truncation-only first-flip truncation. After the search, candidates are evaluated based on SSIM and ℓ_2 thresholds to filter out invalid frontier pairs early on.

In *truncation-assisted style mixing* (Algorithm 1), for each seed z , we first render the untruncated baseline $x_{1.0} = G(z, c; 1.0)$ and select the top- K rival classes R by classifier confidence. For each truncation budget $b \in B$, we then render a truncated source image $x_b = G(z, c; b)$ and, for each rival $r \in R$, style-mix the source-class latent $w_c^{(b)}$ with the rival latent $w_r^{(b)}$ over a specified set of layers L [18]. We run a binary search over the mixing weight $\lambda \in [0, 1]$ to find the smallest λ that flips the SUT prediction from the source class while keeping the similarity constraints (SSIM and ℓ_2).

Algorithm 1 Testing via Truncation-Assisted Style Mixing

Input. Generator G ; classifier h ; truncation budgets B (ψ_T); seeds \mathcal{Z} ; top- K rivals; layers L ; binary-search steps T ; SSIM and ℓ_2 threshold τ .

Output. A set of recorded frontiers with metadata $(x_b, x_\lambda, b, \lambda)$.

- (1) For each seed $z \in \mathcal{Z}$:
 - (a) Render baseline: $x_{1.0} \leftarrow G(z, c; 1.0)$.
 - (b) Let $R \leftarrow$ the top- K rival classes by confidence on $x_{1.0}$.
 - (c) For each truncation budget $b \in B$:
 - (i) Render truncated source: $x_b \leftarrow G(z, c; b)$.
 - (ii) For each rival $r \in R$:
 - (A) Run a binary search over $\lambda \in [0, 1]$ (for T steps). At each step, generate $x_\lambda \leftarrow \text{StyleMix}(w_c^{(b)}, w_r^{(b)}, L, \lambda)$.
 - (B) If x_λ satisfies the similarity constraints (SSIM and ℓ_2) w.r.t. x_b and $\arg \max h(x_\lambda) \neq c$, then record the frontier $(x_b, x_\lambda, b, \lambda)$ and stop iterating rivals for this (z, b) .
 - (2) Aggregate all recorded frontiers and store the corresponding JSON files.

Algorithm 2 Truncation-Only First-Flip Search

Input. Generator G ; classifier h ; class c ; schedule $\Psi = \{1.0, \psi_2, \dots, \psi_M\}$ (descending); seeds \mathcal{Z} .

Output. Recorded frontiers (z, c, x_{ψ^*}) with metadata.

- (1) For each seed $z \in \mathcal{Z}$:
 - (a) Generate baseline input: $x_{1.0} \leftarrow G(z, c; 1.0)$.
 - (b) If $\arg \max h(x_{1.0}) \neq c$, skip this seed.
 - (c) For each truncation level $\psi_T \in \Psi \setminus \{1.0\}$ (in descending order):
 - (i) Generate truncated image: $x_{\psi_T} \leftarrow G(z, c; \psi_T)$.
 - (ii) If $\arg \max h(x_{\psi_T}) \neq c$:
 - (A) Set $\psi^* \leftarrow \psi_T$.
 - (B) Record frontier (z, c, x_{ψ_T}) and ψ^* .
 - (C) Stop iterating truncation levels for this seed.
 - (2) Aggregate all recorded frontiers and export the corresponding JSON files.

In *truncation-only first-flip* (Algorithm 2), for each seed z we first generate a baseline image $x_{1.0} = G(z, c; 1.0)$. We then decrease the truncation parameter ψ along a predefined descending schedule and re-render the image at each step. The search stops at the first ψ^* for which the classifier prediction flips from the source class, and the corresponding truncated image is recorded as a frontier case. Fig. 3 illustrates a truncation-only refinement: a baseline sample that is human-invalid at $\psi=1.00$ becomes human-valid at $\psi=0.55$ and simultaneously flips to a rival class. This example shows how moderate truncation can raise validity while moving the sample closer to a decision boundary, even without style mixing.

Lowering ψ can also *salvage seeds* that fail the baseline at $\psi = 1.0$, moving them toward regions where they change the SUTs behavior and remain within the perceptual threshold. These salvaged seeds tend to lie closer to decision boundaries, increasing the likelihood of flips. Additionally, truncation reshapes the classifier's confidence landscape, sometimes surfacing rival classes that were suppressed at $\psi = 1.0$, a phenomenon we term *target revelation*. For example, Fig. 4 shows the distribution of ψ^* across human-validated, fault-revealing seeds in MNIST, one of the datasets of our study. Fig. 5 illustrates this effect, where decreasing ψ affects the rival confidence and enables a human-valid seed to flip under truncation alone.

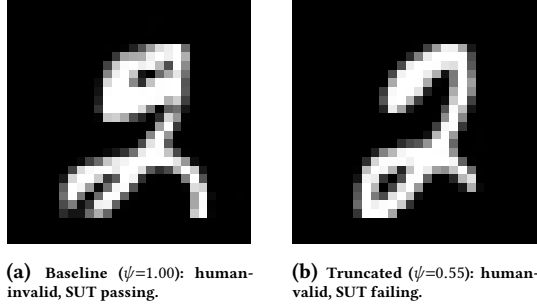


Figure 3: Truncation-only search. Truncation refines a human-invalid baseline into a human-valid image and flips the SUT prediction.

4 Empirical Study

4.1 Research Questions

RQ₁ (effectiveness). *How does truncation affect the validity, diversity, and fault detection of generated test inputs?*

This question evaluates the core trade-off introduced by truncation. Lower truncation levels increase image realism and classifier confidence but may reduce diversity, potentially limiting fault discovery. Understanding this balance is important to selecting truncation settings that maximize both test validity and effectiveness.

RQ₂ (comparison). *How do the style-mixing and first-flip methods compare in terms of efficiency and fault detection?*

This question contrasts two strategies for exploring the latent space: (i) *style-mixing*, which searches along semantic directions via layer-wise interpolation, and (ii) *first-flip*, which relies on truncation descent. Comparing their performance clarifies whether structured latent manipulations are necessary or if truncation alone suffices for generating meaningful, fault-revealing inputs.

4.2 Experimental Setup, Metrics, and Procedure

4.2.1 Objects of Study. We evaluate the proposed approach on three benchmark datasets: MNIST (28×28 grayscale) [24], Fashion MNIST (28×28 grayscale) [46], and CIFAR-10 (32×32 color) [19]. For each dataset, we employ pretrained class-conditional StyleGAN2(-ADA) generators as test input producers from existing work [45]. The corresponding SUTs used are Torchvision baselines: a small CNN for MNIST and Fashion MNIST, and a ResNet-18 for CIFAR-10 [12], also from existing work [45].

Truncation is explored over fixed budgets (1), and an adaptive schedule (2) is used to automatically locate the minimal truncation value ψ^* that produces valid candidates.

In Table 1, experiments on MNIST, Fashion MNIST, and CIFAR-10 show that diversity (mean pairwise LPIPS) dropped sharply at $\psi \in \{0.6, 0.5\}$, and lower values would further reduce diversity without supporting our goal of balancing validity and diversity. For this reason, we set a minimal truncation value at $\psi = 0.5$ in the main experiments.

$$\psi_{\text{fixed}} = \{1.0, 0.9, 0.8, 0.7, 0.6, 0.5\} \quad (1)$$

$$\psi_{\text{adapt}} = \{1.0, 0.95, 0.90, 0.85, 0.80, 0.75, 0.70, 0.60, 0.50\} \quad (2)$$

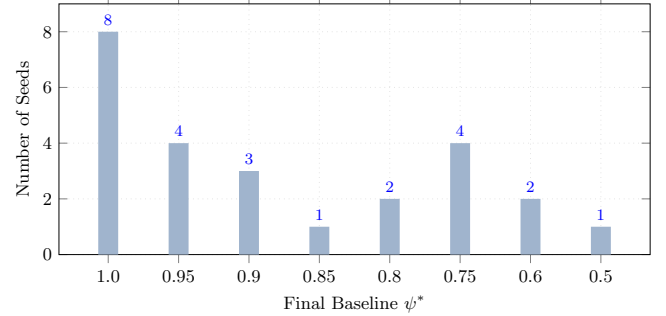


Figure 4: Minimal truncation ψ^* in MNIST ($n = 25$).

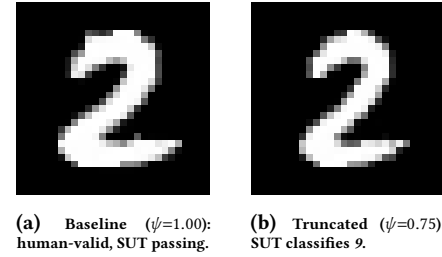


Figure 5: Target revelation via truncation. Lowering ψ causes human-valid seed to flip under truncation alone.

Each generator is evaluated with 20 latent seeds per class for MNIST and Fashion MNIST, and 30 seeds per class for CIFAR-10. Identical seed lists are reused across budgets for comparability.

4.2.2 Evaluation Metrics. We assess the impact of truncation using four operational metrics that jointly capture the realism, diversity, and fault-revealing power of generated test inputs:

- **Baseline Acceptance.** For a seed z and class c , the baseline image $x_{1,0} = G(z, c; 1.0)$ is accepted if it meets three classifier-based criteria: (1) $\arg \max h(x_{1,0}) = c$ (predicted as the correct class); (2) top-class confidence $p_{(1)} \geq p_{\min}$; (3) confidence margin $p_{(1)} - p_{(2)} \geq \delta$.
- **Screening Validity.** For each truncation level b , the generated image $x_b = G(z, c; b)$ must pass both the classifier gate above and a threshold of $\text{SSIM} = 0.95$ and $\ell_2 = 0.2$ that is fixed for every dataset. This step filters out visually implausible or off-mode samples before human inspection [45].
- **Human-Validated Validity.** Screened images are independently reviewed by human annotators to confirm whether they are class-plausible. This step captures true semantic validity that cannot be guaranteed by automated proxies.
- **Diversity and Fault Detection.** Diversity is quantified as the mean pairwise perceptual distance (LPIPS) among all human-validated samples for a given (c, b) , measuring coverage of the visual input space. Fault detection is the proportion of validated samples that cause a misclassification, i.e., $\arg \max h(x) \neq c$, indicating the generator's ability to reveal model weaknesses [49].

4.2.3 Procedure. For each dataset, we generate test inputs under the fixed and adaptive truncation schedules and apply the two

Table 1: Results across datasets, truncation levels, and probing techniques. Each entry reports the number of sampled seeds, human-validated inputs, validation rate, mean LPIPS, fault detection rate, and efficiency (seeds per validated input).

Dataset	Technique	Setting	Seeds	Human-val	Human-Val. Rate	LPIPS	Fault Rate
MNIST	Style-Mixing	No trunc.	504	11	44%	0.194	2.18%
		$\psi=0.9$	518	12	48%	0.224	2.31%
		$\psi=0.8$	461	16	64%	0.215	3.47%
		$\psi=0.7$	549	14	56%	0.190	2.55%
		$\psi=0.6$	455	20	80%	0.152	4.39%
		$\psi=0.5$	448	17	68%	0.143	3.79%
		Adaptive	161	15	60%	0.252	9.31%
	Truncation-Only	Gradual trunc.	499	19	76%	0.156	3.80%
Fashion MNIST	Style-Mixing	No trunc.	431	23	92%	0.240	5.33%
		$\psi=0.9$	502	24	96%	0.236	4.78%
		$\psi=0.8$	718	25	100%	0.173	3.48%
		$\psi=0.7$	706	25	100%	0.203	3.54%
		$\psi=0.6$	392	24	96%	0.166	6.12%
		$\psi=0.5$	526	25	100%	0.170	4.75%
		Adaptive	169	22	88%	0.214	13.0%
	Truncation-only	Gradual trunc.	93	25	100%	0.227	26.8%
CIFAR-10	Style-Mixing	No trunc.	275	13	52%	0.424	4.72%
		$\psi=0.9$	249	13	52%	0.404	5.22%
		$\psi=0.8$	252	16	64%	0.400	6.34%
		$\psi=0.7$	249	15	60%	0.406	6.02%
		$\psi=0.6$	158	17	68%	0.383	10.7%
		$\psi=0.5$	118	16	64%	0.338	13.5%
		Adaptive	255	13	52%	0.421	5.09%
	Truncation-only	Gradual trunc.	266	16	64%	0.386	6.01%

probing methods (*style-mixing* and *truncation-only first-flip*). Each generated image undergoes automated screening and, if accepted, human verification. We then report (i) screening and validation rates per truncation level, (ii) diversity among validated inputs, (iii) fault detection ratios, and (iv) the relative efficiency of the two probing methods. Together, these measurements allow us to analyze how truncation affects the trade-off between *validity*, *diversity*, and *fault revelation*, and to assess whether adaptive truncation or specific probing strategies offer systematic advantages.

4.2.4 Human Validation. To obtain human validity, we conducted a small-scale annotation with two assessors. For each dataset and class, we prepared a folder containing generated flipped test cases and removed all metadata about their origin (e.g., truncation level ψ , generation technique, and classifier outputs). Annotators therefore only saw images and their source classes. They were instructed to answer a binary question: “*Is this image a valid example of this class?*” (yes/no). We marked an image as *human-valid* if the annotator answered “yes” to the question. Disagreements were resolved through discussion until consensus was reached.

4.3 Effectiveness (RQ₁)

Table 1 presents the results for all datasets and compared techniques. The results are averaged over the 25 runs. Regarding MNIST, without regularization ($\psi=1.0$), the human-validated rate is 44% (11/25) with a cost of 42.00 seeds per validated case. As ψ decreases, validation improves and effort drops, peaking at $\psi=0.6$ with 80% human-validated pairs. Pushing regularization further to $\psi=0.5$ slightly reduces validation (68%). Similarly, in CIFAR-10 results of human validation is highest at $\psi=0.6$ and slightly decreases at $\psi=0.5$, while in Fashion MNIST human validation peaks at $\psi=0.5$.

The *adaptive* strategy achieves the best efficiency: it reaches 15 human-validated pairs using only 161 seeds in total, less than half of the effort required than at $\psi=0.6$. This confirms the practical value of per-seed regularization: instead of discarding borderline seeds at $\psi=1.0$, adaptively “salvaging” them near ψ^* yields more fault-prone tests at lower cost (see Fig. 6). We observed a similar result in Fashion MNIST, where seed usage dropped from 526 (highest human validation) at $\psi=0.6$ to 161. While the adaptive strategy also decreased seed usage in CIFAR-10, the reduction was not as significant as in MNIST and Fashion MNIST.

Although Table 1 primarily reports acceptance/efficiency, qualitative inspection in Fig. 6 shows that $\psi \approx 0.6$ maintains sufficient visual spread to reveal decision-boundary behavior. Extremely low

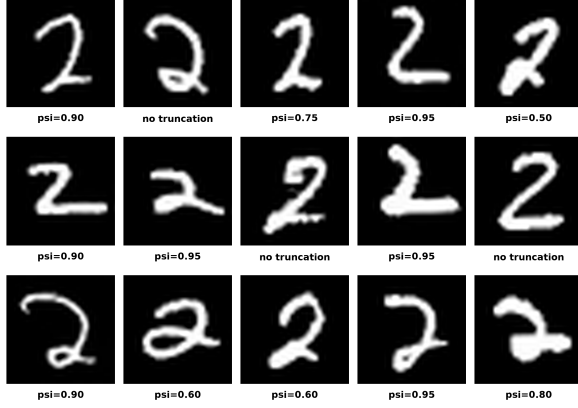


Figure 6: MNIST: adaptive truncation, human-validated, fault-revealing test cases.

ψ would risk collapsing diversity; our results suggest that mild to moderate regularization (and especially the adaptive strategy) strikes a better balance between human-validated realism and the variety needed to expose faults. Similar reasoning applies to the other datasets.

RQ₁ (effectiveness). Mild–moderate latent regularization ($\psi \approx 0.6$) maximizes human-validated frontier yield on MNIST. The adaptive policy minimizes human effort (seeds/valid) by salvaging hard seeds. Qualitative analysis shows that diversity remains adequate at these settings to expose faults, whereas overly strong regularization offers lower returns.

4.4 Comparison (RQ₂)

The two strategies appear to be complementary. *First-flip* is light-weight and effective for quickly revealing faults under a truncation schedule (see Fig. 7); *style-mixing* provides semantically guided boundary traversal with finer control, at the cost of extra search (see Fig. 6).

Across the same truncation settings used for RQ₁, *truncation-only first-flip* requires fewer design choices (no rival selection or layer sets) and rapidly identifies misbehaviours by descending ψ . This makes it a strong configuration when computing time is limited. *Style-mixing*, in contrast, steers the latent representation toward specific rival classes via layer-wise interpolation and binary search; this extra complexity typically yields cleaner, semantically interpretable boundary crossings and can improve human acceptance for borderline cases, but incurs additional tuning (layers L , step budget T , rival selection).

On MNIST, runs that reached the fixed quota of 25 frontiers showed that *truncation-only first-flip* benefited markedly from adaptive seed salvage (lower seeds/valid) and produced a higher fraction of validated faults in our MNIST experiments, while *style-mixing* produced boundary examples with more controllable semantics.

On Fashion MNIST, truncation-only first-flip achieves the lowest seed usage (93 seeds for 25 validated faults) and the highest fault

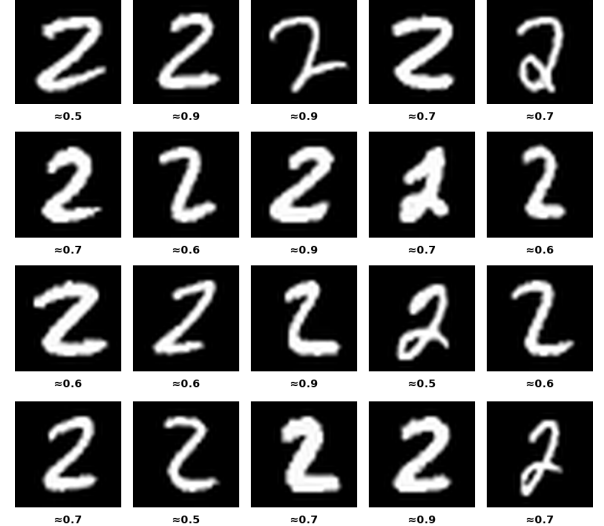


Figure 7: Cases from MNIST where the first flip occurs at ψ^* .

detection rate, making it the most efficient option. In contrast, *style-mixing* configurations require more seeds but allow finer control over semantic edits.

On CIFAR-10, the distinction between the two techniques is less significant. Truncation-only first-flip remains competitive in fault detection, but its advantage over *style-mixing* is smaller than on Fashion MNIST, indicating that dataset characteristics influence how strongly each technique benefits from the first-flip technique. In short, if the goal is *fast fault surfacing*, first-flip under adaptive ψ is preferable; if the goal includes *interpretable semantics* for analysis and debugging, *style-mixing* provides control at a moderate additional cost.

RQ₂ (comparison). First-flip is the most efficient for fault discovery under latent regularization; style-mixing complements it by adding semantic control over boundary direction.

4.5 Threats to Validity

4.5.1 Internal validity. A potential threat arises from the choice of latent seeds, as some seeds may inherently yield more realistic or diverse samples. We mitigate this by reusing identical seed lists across all truncation budgets and probing methods. Strong truncation may also induce mode collapse, reducing diversity and artificially inflating validity; to limit this effect, we restrict truncation sweeps to $\psi \geq 0.5$. In addition, the degree of latent disentanglement varies across datasets and classes, which can make the effects of truncation or layer-wise edits less consistent. This reflects an intrinsic limitation of current generative models rather than an artifact of our setup.

Our human-validity labels are based on a small-scale annotation with two assessors and therefore introduce subjectivity. We treat this step as a lightweight plausibility filter and interpret it jointly with automated screening, diversity, and fault-detection metrics. Similarly, the LPIPS metric used for filtering is only an approximation of semantic similarity, but it provides a consistent



Figure 8: Layer-specific truncation sweeps (same seed). Columns show decreasing ψ from 1.0 to 0.1; rows indicate which layers are truncated: up to layer 2 (coarse), up to layer 5 (coarse+middle), and up to layer 8 (all layers).

and reproducible basis for comparing truncation levels and probing strategies.

4.5.2 External validity. Experiments are conducted on small-scale image datasets with relatively simple classifiers, and the observed relationships between truncation, validity, and diversity may not directly transfer to larger or more complex domains. Moreover, our conclusions apply specifically to StyleGAN-based generators; truncation may behave differently in other architectures, such as diffusion or transformer-based models. Extending this analysis to additional modalities and generative paradigms is an important direction for future work.

To ensure transparency and replicability, we release all experimental scripts (including seed lists and fixed-noise configurations), JSON logs, and plotting templates required to reproduce every figure and table in our replication package [1].

5 Discussion

Our results show that truncation can serve as a simple yet effective control for enhancing the quality of generated test inputs in latent-space testing frameworks such as MIMICRY. Moderate truncation levels ($\psi \approx 0.6$) tend to maximize the fraction of human-validated valid and fault-revealing test cases, striking a balance between semantic realism and diversity.

The adaptive truncation mechanism further improves efficiency by salvaging seeds that would otherwise be discarded, leading to a richer and more fault-prone test pool. This adaptivity makes truncation-based refinement particularly suitable when annotation or computational budgets are limited.

Between the two probing methods, *style-mixing* provides structured, semantically meaningful perturbations but requires additional computation and hyperparameter tuning. In contrast, the *truncation-only first-flip* approach offers a lightweight, diagnostic alternative that can reveal classifier weaknesses with minimal setup. Combining both techniques allows a comprehensive exploration of decision boundaries, from coarse latent refinements to fine-grained semantic traversals.

In addition to ψ , StyleGAN exposes adjacent controls that plausibly affect test case validity and diversity: (i) per-layer truncation cutoffs that restrict where truncation is applied in \mathcal{W}^+ , (ii) the magnitude/schedule of stochastic noise injection in the synthesis network, and (iii) the choice of layers used for style mixing [18].

6 Conclusion and Future Work

This study investigated how truncation—a common latent-space regularization technique—affects the generation of test inputs for deep learning classifiers. We quantified its impact on human-verified validity, diversity, and fault detection, and introduced a simple yet effective *first-flip* probe based solely on truncation. We further compared this approach with a truncation-assisted *style-mixing* probe that explores the latent space through semantic interpolation.

Our findings show that moderate truncation levels and adaptive seed refinement yield the best balance between validity, diversity, and fault revelation. These results provide practical guidance and actionable defaults for configuring generative test input generators, as well as a reproducible protocol to support future research in deep learning testing.

In our experiments, we focus on StyleGAN, but similar fidelity controls appear in other generative architectures, such as guidance in diffusion models and temperature, top- k , and top- p in autoregressive decoders. The same sample-and-screen design can be reused to calibrate these knobs in diffusion or transformer-based generators to balance the fidelity–diversity trade-off. We leave validation of this generalization to future work.

Future extensions of this study could explore truncation effects across StyleGAN’s layers as shown in Fig. 8, as well as related generator-level controls such as synthesis noise or layer-selection choices, and in more complex generative architectures, such as diffusion or transformer-based models, where latent representations and fidelity controls differ fundamentally from GANs. Finally, integrating automated validity estimation and adaptive truncation scheduling could reduce reliance on human annotation, advancing scalable and self-adaptive test generation for AI-based systems.

References

- [1] 2026. Replication Package. <https://github.com/ast-fortiss-tum/frontier-generation-latent-space-interpolation>.
- [2] David Bau, Jun-Yan Zhu, Hendrik Strobelt, Bolei Zhou, Joshua B. Tenenbaum, William T. Freeman, and Antonio Torralba. 2018. GAN Dissection: Visualizing and Understanding Generative Adversarial Networks. *arXiv preprint arXiv:1811.10597* (2018).
- [3] Wieland Brendel, Jonas Rauber, and Matthias Bethge. 2018. Decision-Based Adversarial Attacks: Reliable Attacks Against Black-Box Machine Learning Models. In *Proc. ICLR*.
- [4] Andrew Brock, Jeff Donahue, and Karen Simonyan. 2019. Large Scale GAN Training for High Fidelity Natural Image Synthesis. In *Proc. ICLR*.
- [5] Jianbo Chen, Michael I. Jordan, and Martin J. Wainwright. 2020. HopSkipJumpAttack: A Query-Efficient Decision-Based Attack. In *Proceedings of the IEEE Symposium on Security and Privacy (S&P)*.
- [6] Xingcheng Chen, Matteo Biagiola, Vincenzo Riccio, Marcelo d'Amorim, and Andrea Stocco. 2025. XMutant: XAI-based Fuzzing for Deep Learning Systems. In *Empirical Software Engineering* (2025).
- [7] Swaroopa Dola, Rory McDaniel, Matthew B Dwyer, and Mary Lou Soffa. 2024. Cit4dnn: Generating diverse and rare inputs for neural networks using latent space combinatorial testing. In *Proceedings of the IEEE/ACM 46th International Conference on Software Engineering*. 1–13.
- [8] Yuan Gao, Mattia Piccinini, Yuchen Zhang, Dingrui Wang, Korbinian Moller, Roberto Brusnicki, Baha Zarrouki, Alessio Gambi, Jan Frederik Totz, Kai Storms, Steven Peters, Andrea Stocco, Bassam Alrifaei, Marco Pavone, and Johannes Betz. 2025. Foundation Models in Autonomous Driving: A Survey on Scenario Generation and Scenario Analysis. *arXiv:2506.11526* [cs.RO]. <https://arxiv.org/abs/2506.11526>
- [9] Ian Goodfellow, Jean Pouget-Abadie, Mehdi Mirza, Bing Xu, David Warde-Farley, Sherjil Ozair, Aaron Courville, and Yoshua Bengio. 2014. Generative Adversarial Nets. In *Proc. NeurIPS*.
- [10] Ruben Grewal, Paolo Tonella, and Andrea Stocco. 2024. Predicting Safety Misbehaviours in Autonomous Driving Systems using Uncertainty Quantification. In *Proceedings of 17th IEEE International Conference on Software Testing, Verification and Validation (ICST '24)*. IEEE, 12 pages.
- [11] Jianmin Guo, Yao Shen, Yue Huang, et al. 2019. DLFuzz: Differential Fuzzing Testing of Deep Learning Systems. In *Proc. ICSE*.
- [12] Kaiming He, Xiangyu Zhang, Shaoqing Ren, and Jian Sun. 2016. Deep Residual Learning for Image Recognition. In *Proc. CVPR*.
- [13] Martin Heusel, Hubert Ramsauer, Thomas Unterthiner, Bernhard Nessler, and Sepp Hochreiter. 2017. GANs Trained by a Two Time-Scale Update Rule Converge to a Local Nash Equilibrium. In *Proc. NeurIPS*.
- [14] Nargiz Humbatova, Gunel Jahangirova, Gabriele Bavota, Vincenzo Riccio, Andrea Stocco, and Paolo Tonella. 2020. Taxonomy of Real Faults in Deep Learning Systems. In *Proceedings of 42nd International Conference on Software Engineering (Seoul, Republic of Korea) (ICSE '20)*. ACM, New York, NY, USA, 12 pages. [doi:10.1145/3377811.3380395](https://doi.org/10.1145/3377811.3380395)
- [15] Erik Härkönen, Aaron Hertzmann, Jaakko Lehtinen, and Sylvain Paris. 2020. GANSpace: Discovering Interpretable GAN Controls. In *Proc. NeurIPS*.
- [16] Sungmin Kang, Robert Feldt, and Shin Yoo. 2020. SINVAD: Search-based Image Space Navigation for DNN Image Classifier Test Input Generation. In *Proc. ISSTA*. ACM, 521–528. [doi:10.1145/3387940.3391456](https://doi.org/10.1145/3387940.3391456)
- [17] Tero Karras, Miika Aittala, Janne Hellsten, et al. 2021. Alias-Free Generative Adversarial Networks. In *Proc. NeurIPS*. *NeurIPS*.
- [18] Tero Karras, Samuli Laine, and Timo Aila. 2019. A Style-Based Generator Architecture for Generative Adversarial Networks. In *Proc. CVPR*.
- [19] Alex Krizhevsky. 2009. *Learning Multiple Layers of Features from Tiny Images*. Technical Report. University of Toronto.
- [20] Tuomas Kynkänniemi, Tero Karras, Samuli Laine, Jaakko Lehtinen, and Timo Aila. 2019. Improved Precision and Recall Metric for Assessing Generative Models. In *Proc. NeurIPS*.
- [21] Stefano Carlo Lambertenghi, Hannes Leonhard, and Andrea Stocco. 2025. Benchmarking Image Perturbations for Testing Automated Driving Assistance Systems. In *Proceedings of the 18th IEEE International Conference on Software Testing, Verification and Validation (ICST '25)*. IEEE, 12 pages.
- [22] Stefano Carlo Lambertenghi and Andrea Stocco. 2024. Assessing Quality Metrics for Neural Reality Gap Input Mitigation in Autonomous Driving Testing. In *2024 IEEE Conference on Software Testing, Verification and Validation (ICST '24)*. IEEE, 173–184. [doi:10.1109/ICST60714.2024.00024](https://doi.org/10.1109/ICST60714.2024.00024)
- [23] Stefano Carlo Lambertenghi, Mirena Flores Valdez, and Andrea Stocco. [n. d.]. A Multi-Modality Evaluation of the Reality Gap in Autonomous Driving Systems. In *Proceedings of ASE '25*. IEEE.
- [24] Yann LeCun, Léon Bottou, Yoshua Bengio, and Patrick Haffner. 1998. Gradient-Based Learning Applied to Document Recognition. *Proc. IEEE* 86, 11 (1998), 2278–2324.
- [25] Lei Ma, Felix Juefei-Xu, Fuyuan Zhang, et al. 2018. DeepGauge: Multi-Granularity Testing Criteria for Deep Learning Systems. In *Proc. ASE (Montpellier, France) (ASE 2018)*. ACM, New York, NY, USA, 120–131. [doi:10.1145/3238147.3238202](https://doi.org/10.1145/3238147.3238202)
- [26] Maryam Maryam, Matteo Biagiola, Andrea Stocco, and Vincenzo Riccio. 2025. Benchmarking Generative AI Models for Deep Learning Test Input Generation. In *2025 IEEE Conference on Software Testing, Verification and Validation (ICST)*. IEEE, 174–185.
- [27] Seyed-Mohsen Moosavi-Dezfooli, Alhussein Fawzi, and Pascal Frossard. 2016. DeepFool: A Simple and Accurate Method to Fool Deep Neural Networks. In *Proc. CVPR*.
- [28] Nusrat Jahan Mozumder, Felipe Toledo, Swaroopa Dola, and Matthew B Dwyer. 2025. RBT4DNN: Requirements-based Testing of Neural Networks. *arXiv preprint arXiv:2504.02737* (2025).
- [29] Augustus Odena, Catherine Olsson, David G. Andersen, and Ian Goodfellow. 2018. TensorFuzz: Debugging Neural Networks with Coverage-Guided Fuzzing. *arXiv preprint arXiv:1807.10875* (2018).
- [30] Kexin Pei, Yinzhi Cao, Junfeng Yang, and Suman Jana. 2017. DeepXplore: Automated Whitebox Testing of Deep Learning Systems. In *Proc. SOSR (Shanghai, China)*. *Commun. ACM* 62, 11, 1–18. [doi:10.1145/3132747.3132785](https://doi.org/10.1145/3132747.3132785)
- [31] Vincenzo Riccio, Gunel Jahangirova, Andrea Stocco, Nargiz Humbatova, Michael Weiss, and Paolo Tonella. 2020. Testing machine learning based systems: a systematic mapping. *Empirical Software Engineering* 25 (2020), 5193–5254.
- [32] Vincenzo Riccio and Paolo Tonella. 2020. Model-Based Exploration of the Frontier of Behaviour for Deep Learning System Testing. In *Proc. ESEC/FSE*. ACM, 876–888. [doi:10.1145/3368089.3409730](https://doi.org/10.1145/3368089.3409730)
- [33] Mehdi S. M. Sajjadi, Olivier Bachem, and Mario Lucic. 2018. Assessing Generative Models via Precision and Recall. In *Proc. NeurIPS*.
- [34] Tim Salimans, Ian Goodfellow, Wojciech Zaremba, Vicki Cheung, Alec Radford, and Xi Chen. 2016. Improved Techniques for Training GANs. In *Proc. NeurIPS*.
- [35] Axel Sauer, Katja Schwarz, and Andreas Geiger. 2022. StyleGAN-XL: Scaling StyleGAN to Large Datasets. In *Proc. SIGGRAPH*. 1–10.
- [36] Yujun Shen and Bolei Zhou. 2021. Closed-Form Factorization of Latent Semantics in GANs. In *Proc. CVPR*.
- [37] Andrea Stocco, Paulo J. Nunes, Marcelo d'Amorim, and Paolo Tonella. 2022. ThirdEye: Attention Maps for Safe Autonomous Driving Systems. In *Proceedings of 37th IEEE/ACM International Conference on Automated Software Engineering (ASE '22)*. IEEE/ACM. [doi:10.1145/3551349.3556968](https://doi.org/10.1145/3551349.3556968) Accepted.
- [38] Andrea Stocco, Brian Pulfer, and Paolo Tonella. 2022. Mind the Gap! A Study on the Transferability of Virtual vs Physical-world Testing of Autonomous Driving Systems. *IEEE Transactions on Software Engineering* 04 (apr 2022), 1928–1940. [doi:10.1109/TSE.2022.3202311](https://doi.org/10.1109/TSE.2022.3202311)
- [39] Andrea Stocco, Brian Pulfer, and Paolo Tonella. 2023. Model vs System Level Testing of Autonomous Driving Systems: A Replication and Extension Study. *Empirical Softw. Engng.* 28, 3 (may 2023), 73. [doi:10.1007/s10664-023-10306-x](https://doi.org/10.1007/s10664-023-10306-x)
- [40] Andrea Stocco and Paolo Tonella. 2020. Towards Anomaly Detectors that Learn Continuously. In *Proceedings of 31st International Symposium on Software Reliability Engineering Workshops (ISSREW 2020)*. IEEE.
- [41] Andrea Stocco and Paolo Tonella. 2021. Confidence-driven Weighted Retraining for Predicting Safety-Critical Failures in Autonomous Driving Systems. *Journal of Software: Evolution and Process* (2021). [doi:10.1002/smр.2386](https://doi.org/10.1002/smr.2386)
- [42] Andrea Stocco, Michael Weiss, Marco Calzana, and Paolo Tonella. 2020. Misbehaviour Prediction for Autonomous Driving Systems. In *Proceedings of 42nd International Conference on Software Engineering (ICSE '20)*. ACM, 12 pages.
- [43] Yuchi Tian, Kexin Pei, Suman Jana, and Baishakhi Ray. 2018. DeepTest: Automated Testing of Deep-Neural-Network-Driven Autonomous Cars. In *Proc. ICSE*.
- [44] Michael Weiss, André García Gómez, and Paolo Tonella. 2023. Generating and detecting true ambiguity: a forgotten danger in DNN supervision testing. *Empirical Softw. Engng.* 28, 6 (nov 2023), 36 pages. [doi:10.1007/s10664-023-10393-w](https://doi.org/10.1007/s10664-023-10393-w)
- [45] Oliver Weiβl, Amr Abdellatif, Xingcheng Chen, Giorgi Merabishvili, Vincenzo Riccio, Severin Kacianka, and Andrea Stocco. 2025. Targeted Deep Learning System Boundary Testing. *ACM Trans. Softw. Eng. Methodol.* (Oct. 2025). [doi:10.1145/3771557](https://doi.org/10.1145/3771557)
- [46] Han Xiao, Kashif Rasul, and Roland Vollgraf. 2017. Fashion-MNIST: A Novel Image Dataset for Benchmarking Machine Learning Algorithms. *arXiv preprint arXiv:1708.07747* (2017).
- [47] Xiaofei Xie, Lei Ma, Felix Juefei-Xu, et al. 2019. DeepHunter: A Coverage-Guided Fuzz Testing Framework for Deep Neural Networks. In *Proc. ISSTA*.
- [48] Mengshi Zhang, Yuqun Zhang, Lingming Zhang, Cong Liu, and Sarfraz Khurshid. 2018. DeepRoad: GAN-Based Metamorphic Testing and Input Validation Framework for Autonomous Driving Systems. In *Proc. ASE*. ACM. [doi:10.1145/3238147.3238187](https://doi.org/10.1145/3238147.3238187)
- [49] Richard Zhang, Phillip Isola, Alexei A. Efros, et al. 2018. The Unreasonable Effectiveness of Deep Features as a Perceptual Metric. In *Proc. CVPR*.
- [50] Tahereh Zohdinasab, Vincenzo Riccio, Alessio Gambi, and Paolo Tonella. 2021. DeepHyperion: Exploring the Feature Space of Deep Learning-Based Systems through Illumination Search. In *Proc. ISSTA (ISSTA '21)*. ACM, 79–90. [doi:10.1145/3460319.3464811](https://doi.org/10.1145/3460319.3464811)
- [51] Tahereh Zohdinasab, Vincenzo Riccio, Alessio Gambi, and Paolo Tonella. 2023. Efficient and Effective Feature Space Exploration for Testing Deep Learning Systems. *ACM Transactions on Software Engineering and Methodology* 32, 2 (2023), 49:1–49:38. [doi:10.1145/3544792](https://doi.org/10.1145/3544792)